Arginase 1–Based Immune Modulatory Vaccines Induce Anticancer Immunity and Synergize with Anti–PD-1 Checkpoint Blockade

Mia Aaboe Jørgensen[1], Stefano Ugel[2], Mie Linder Hübbe[1], Marco Carretta[1], Maria Perez-Penco[1], Stine Emilie Weis-Banke[1], Evelina Martinenaite[1,3], Katharina Kopp[3], Marion Chapellier[3], Annalisa Adamo[2], Francesco De Sanctis[2], Cristina Frusteri[2], Manuela Iezzi[4], Mai-Britt Zocca[3], Daniel Hargbøll Madsen[1], Ayako Wakatsuki Pedersen[3], Vincenzo Bronte[2], and Mads Hald Andersen[1,3,5]

ABSTRACT

Expression of the L-arginine catabolizing enzyme arginase 1 (ARG1) is a central immunosuppressive mechanism mediated by tumor-educated myeloid cells. Increased activity of ARG1 promotes the formation of an immunosuppressive microenvironment and leads to a more aggressive phenotype in many cancers. Intrinsic T-cell immunity against ARG1-derived epitopes in the peripheral blood of cancer patients and healthy subjects has previously been demonstrated. To evaluate the antitumor efficacy of ARG1-derived peptide vaccines as a monotherapy and as a combinational therapy with checkpoint blockade, different *in vivo* syngeneic mouse tumor models were utilized. To evaluate the antitumor effects, flow cytometry analysis and IHC were performed on tumors, and ELISPOT assays were performed to characterize immune responses. We show that ARG1-targeting therapeutic vaccines were able to activate endogenous antitumor immunity in several *in vivo* syngeneic mouse tumor models and to modulate the cell composition of the tumor microenvironment without causing any associated side effects or systemic toxicity. ARG1-targeting vaccines in combination with anti–PD-1 also resulted in increased T-cell infiltration, decreased ARG1 expression, reduced suppressive function of tumor-educated myeloid cells, and a shift in the M1/M2 ratio of tumor-infiltrating macrophages. These results indicated that the induced shift toward a more proinflammatory microenvironment by ARG1-targeting immunotherapy favors effective tumor control when combined with anti–PD-1 checkpoint blockade. Our data illustrate the ability of ARG1-based immune modulatory vaccination to elicit antigen-specific immunosurveillance and imply the feasibility of this novel immunotherapeutic approach for clinical translation.

Introduction

Cancer cells can directly inhibit anticancer immune mechanisms and corrupt immune cells to generate and uphold an immunosuppressive microenvironment. To evade immune surveillance, tumor cells can promote recruitment of myeloid-derived suppressor cells (MDSC) or differentiation of tumor-associated macrophages (TAM), which together contribute to impairing anticancer immunity through various mechanisms (1–3). Indeed, MDSCs and TAMs inhibit the activation, proliferation, and cytotoxicity of effector T cells and natural killer cells, as well as induce the differentiation and expansion of regulatory T cells (Treg). One of the most effective mechanisms exploited by MDSCs/TAMs for inhibiting T-cell fitness and activation is the aberrant consumption of essential amino acids such as tryptophan, cysteine, and L-arginine in the tumor microenvironment (4). Arginase 1 (ARG1) is expressed by MDSCs and TAMs and catalyzes the conversion of the amino acid L-arginine into L-ornithine and urea. Many studies have shown increased ARG1 activity in cancer, including head and neck cancer (5), breast cancer (6), renal cell carcinoma (7), and non–small cell lung cancer (8), and cancer cells can express ARG1 (9). Unsurprisingly, numerous approaches to inhibit ARG1 have been developed, and ARG1 inhibitors have shown promising results in different mouse models (10, 11). For instance, an ARG1 inhibitor was shown to block tumor growth in a mouse lung carcinoma model with a subpopulation of mature tumor-associated myeloid cells that express high ARG1 (10); analogously, ARG1 transcriptional inhibition by either AT38 ([3-(aminocarbonyl) furoxan-4-yl] methyl salicylate; ref. 12) or phosphodiesterase 5 inhibitors (13) increases the therapeutic impact of immunotherapy. Finally, genetic knockout of ARG1 improves survival in tumor-bearing mice receiving adoptive transfer of tumor-specific cytotoxic T cells (14).

We speculated on the possibility to evoke an immune response against ARG1 to limit the expansion of immunosuppressive elements in the tumor microenvironment. Our previous data report the existence of intrinsic T-cell immunity against ARG1-derived antigens in the peripheral blood of both cancer patients and healthy subjects (15–17), suggesting the presence of an endogenous T-cell receptor (TCR) repertoire toward ARG1 epitopes that can be utilized by immunotherapy. Indeed, ARG1-specific T cells specifically recognized ARG1-expressing immune cells in an ARG1-dependent manner (15), and the T-cell responses against ARG1 were part of the T-cell

[1]National Center for Cancer Immune Therapy (CCIT-DK), Department of Oncology, Copenhagen University Hospital, Herlev, Denmark. [2]Immunology Section, Department of Medicine, University of Verona, Verona, Italy. [3]IO Biotech ApS, Copenhagen, Denmark. [4]Center for Advanced Studies and Technology (CAST), Department of Neurosciences Imaging and Clinical Sciences, University of G. D'Annunzio of Chieti-Pescara, Chieti, Italy. [5]Department of Immunology and Microbiology, University of Copenhagen, Copenhagen, Denmark.

Note: Supplementary data for this article are available at Cancer Immunology Research Online (http://cancerimmunolres.aacrjournals.org/).

V. Bronte and M.H. Andersen contributed equally to this article and share senior authorship.

Corresponding Author: Mads Hald Andersen, National Center for Cancer Immune Therapy (CCIT-DK), 54P4, Herlev Hospital, Borgmester Ib Juuls Vej 25C, Herlev, 2730 Denmark. E-mail: mads.hald.andersen@regionh.dk

Cancer Immunol Res 2021;9:1316–26

doi: 10.1158/2326-6066.CIR-21-0280

memory repertoire (17). To further extend our understanding of the role of ARG1-specific T cells, we examined the possibility to activate and expand *in vivo* ARG1-specific T cells by peptide-based vaccination. We also evaluated the effectiveness of this treatment in controlling tumor progression, either alone or in combination with checkpoint blockade targeting programmed cell death protein 1 (PD-1).

Materials and Methods

Animals

Female C57BL/6 mice were either of own breeding (CCIT-DK, 10–18 weeks old), purchased from Taconic (8–12 weeks old) or Charles River Laboratories Inc. Female BALB/c mice were purchased from Charles River Laboratories Inc. OT-1 TCR transgenic mice (C57BL/6-Tg (TcraTcrb)1100Mjb/J) and CD45.1^{+} congenic mice (B6.SJL-Ptrca-Pepcb/BoyJ) were purchased from Jackson Laboratories. All animal work was conducted under the approval of either the Danish Ethics Committee on experimental animal welfare and performed according to the Danish guidelines or approved by Verona University Ethical Committee according to the Italian guidelines (protocol no. 12722 approved by the Ministerial Decree No. 14/2012-B of January 18, 2012, and protocol no. BR15/08 approved by the Ministerial Decree No. 925/2015-PR of August 28, 2015). For both facilities, all animal experiments were conducted according to the guidelines of Federation of European Laboratory Animal Science Association (FELASA) and ARRIVE, European laws and regulations, and in accordance with the Amsterdam Protocol on animal protection and welfare. Mice were monitored daily and euthanized when displaying excessive discomfort; for example, decreased activity, piloerection, and an ungroomed appearance.

Peptides

Six different 8 mer–20 mer ARG1 peptides (mARG29, mARG56, mARG212, mARG290, $ARG1_{261–280}$, and $ARG1_{191–210}$) and were predicted from the murine (Q61176) and human (P05089) sequence using the prediction server from the University of Tübingen (available at http://www.syfpeithi.de/bin/MHCServer.dll/EpitopePrediction.htm) or by manual screening of the sequence (15). Of these six peptides, only $ARG1_{261–280}$ was shared between the murine and human sequences of ARG1, and only $ARG1_{191–210}$ was predicted from the human sequence. $ARG1_{261–280}$ (TEEIYKTGLLSGLDIMEVNP), $ARG1_{191–210}$ (KTLGIKYFSMTEVDRLGIGK), mARG212 (MEETFSYL), and mARG290 (KSTVNTAVAL) were all reconstituted in 10 mmol/L DMSO. mARG56 (VDVPNDSSF) and mARG29 (AALRKAGLL) were reconstituted in 2 mmol/L H_2O. Peptides were purchased at Schäfer or Pepscan. Ovalbumin ($OVA_{257–264}$, SIINFEKL), the influenza virus hemagglutinin ($HA_{512–520}$, IYSTVASSL), or vehicle for peptide in Montanide ISA 51 VG (Seppic, cat. no. 36362Z) emulsion served as a control vaccine. Control peptides were purchased from JPT Peptide Technologies.

Tumor cell lines and subcutaneous tumor models

The following tumor cell lines were used for the studies reported in this paper: MC38, B16F10, CT26, and MCA205. MC38 and B16F10 were acquired from the NCI–DCTD Repository (NIH, Frederick, MD) in 2016. The mouse CT26 colon cell line was purchased from ATCC (CRL-2638) in 2019, whereas the mouse fibrosarcoma MCA205 cell line was received as a gift from Dr. Laurence Zitvogel (Institut Gustave Roussy, Université de Paris Saclay, INSERM) in 2017. Cell lines were thawed from primary stocks maintained under liquid nitrogen and cultured for a maximum of 3 weeks, during which time all experiments were performed. Cell cultures were regularly tested for *Mycoplasma* using the MycoAlert LookOut Mycoplasma PCR Detection Kit (Sigma-Aldrich). The cell lines have not been authenticated after acquisition.

An inoculum of 5×10^5 or 8×10^5 tumor cells were injected subcutaneously (s.c.) on the right flank in 100 μL DMEM media (Life Technologies; cat. no. 31966-047). After tumor inoculation, treatment with subcutaneous vaccines and anti–PD-1 therapy were initiated as indicated in figures. MC38 tumor cells were cultured in DMEM supplemented with 10% heat-inactivated fetal bovine serum (FBS; Invitrogen), 1% streptomycin/penicillin (Life Technologies), 10 mmol/L HEPES (Life Technologies), 0.1 mmol/L nonessential amino acids (Life Technologies), and 1 mmol/L sodium pyruvate. B16-F10 tumor cells were cultured in DMEM supplemented with 10% FBS and 1% streptomycin/penicillin. MCA205 tumor cells and CT26 tumor cells were cultured in DMEM supplemented with 2 mmol/L L-glutamine (Euroclone), 10 mmol/L HEPES (Euroclone), 20 μmol/L β-mercaptoethanol (Sigma-Aldrich), streptomycin (150 U/mL; Euroclone), penicillin (200 U/mL; Euroclone), and 10% FBS (Invitrogen). After thawing, tumor cells were always passaged a maximum of five times before inoculation. Tumor growth was measured three to four times a week using a digital caliper, and tumor sizes are presented as the mean ± the standard error of the mean (SEM). Tumor volume was calculated according to the following equation: $V\,(\mathrm{mm}^3) = (d2 \times D)/2$, where d (mm) and D (mm) are the smallest and largest perpendicular tumor diameters, respectively, assessed by a caliper measurement. The maximum tumor volume allowed by the Danish Ethics Committee for these studies were 1,500 mm^3, and by the Italian regulation 1,700 mm^3 was allowed.

For tumor rechallenge, an inoculum of 5×10^5 MC38 tumor cells was injected s.c. on the left flank in 100 μL DMEM, and tumor growth was assessed as described above. Seven tumor-naïve C57BL/6 mice were used as controls for tumor growth.

Subcutaneous vaccinations

Animals were vaccinated subcutaneously, as indicated in figures, at the base of the tail with 100 μg peptide in DMSO/H_2O in a 1:1 emulsion with Montanide ISA 51 VG or vaccinated using Covax. Covax is based on the combination of an intraperitoneal injection of 100 mg anti-CD40 (FGK45.5, Bio X Cell) with 100 μg peptide in saline at the tail base and 50 mg of imiquimod 5% cream (Aldara 55 cream, Meda) applied on the vaccination site (14).

Anti–PD-1

Animals were treated with anti-mouse PD-1 (clone: RMP1-14, BioSite; cat. no. BE0146), as indicated in figures, intraperitoneally (i.p.) with 250 μg per dose in multiple-dose studies. Anti–PD-1 was diluted to 250 μg/200 μL in phosphate-buffered saline (PBS) and 200 μL were administered per i.p. injection.

Organ and tumor collection and digestion

Spleens and draining lymph nodes (inguinal lymph nodes) were collected immediately after euthanasia and transferred to RPMI-1640 media supplemented with 10% heat-inactivated FBS, streptomycin/penicillin (100 μg/mL), and streptomycin (100 μg/mL). Each organ was processed through a 70-μm cell strainer, and spleens were treated with red blood cell lysis buffer (Qiagen; cat. no. 158904). All organs were washed twice in RPMI-1640 (Sigma-Aldrich; cat. no. R1145-500 mL), 10% FBS, 1% streptomycin/penicillin. Tumors were

collected immediately after euthanasia and transferred to digestion buffer consisting of collagenase type I (2.1 mg/mL; Worthington; cat. no. LS004196) and DNase I (75 μg/mL; Worthington; cat. no. S002139) in RPMI-1640. The tumors were cut into small pieces using scissors and left overnight at 4°C on an end-over-end rotor (18). The following day, the tumors were shaken for 15 minutes at 37°C before they were passed through a 70-μm cell filter and washed in PBS. The tumors were treated with red cell lysis buffer and washed in PBS.

Murine IFNγ ELISPOT assay

ELISPOT plates (Millipore; cat. no. MSIPN4W50) were coated with mouse IFNγ-specific capture antibody (AN18; Mabtech; cat. no. 3321-3-1000) at a concentration of 12 μg/mL in PBS overnight at 4°C. Splenocytes and cells from the draining lymph nodes from C57BL/6 or BALB/c mice were seeded in the ELISPOT wells in triplicates ($8–10 \times 10^5$ splenocytes per well and 6×10^5 cell from the draining lymph nodes per well) with and without the respective ARG1 peptide (5 μmol/L) and incubated overnight. Concanavalin A (5 μmol/L; Sigma-Aldrich; cat. no. C5275) was used as positive controls in all setups. The following day, the cells were discarded, and the wells of the plates were washed with 300 μL PBS using a CAPP Plate Washer before the biotinylated secondary IFNγ antibody (1:1,000; R4-6A2-biotin; Mabtech, cat. no. 3321-6-1000) was added at the concentration of 1 μg/mL in ELISPOT buffer (PBS, 0.5% BSA and NaN_3) for 2 hours at room temperature. The plates were washed again before addition of streptavidin-AP (1:1,000; Mabtech, cat. no. 3310-10) for 1 hour at room temperature and washed for the last time before the enzyme substrate BCIP/NBT (Mabtech; cat. no. 3650-10) was added to the wells at room temperature for 1 to 5 minutes to visualize IFNγ-secreting cells. The spots were counted using the CTL ImmunoSpot S6 Ultimate-V analyzer with ImmunoSpot software, version 5.1. For phenotyping of $CD4^+$ and $CD8^+$ T cells using IFNγ ELISPOT, $CD4^+$ cells were initially sorted using CD4 (L3T4) microbeads (Miltenyi MACS; cat. no. 130-117-043) for positive selection of $CD4^+$ T cells. $CD8^+$ cells were sorted from the CD4-negative fraction using CD8a (Ly-2) microbeads (Miltenyi MACS; cat. no. 130-117-044). For antigen-presenting cells, splenocytes from C57BL/6 mice were added to a concentration of 2:1 to the $CD4^+$/$CD8^+$ cells in the ELISPOT wells. All samples were performed in technical triplicates, and all ELISPOT data were normalized to 10^6 cells.

Flow cytometry analysis

Antibodies to CD45-PE/Cy7 (cat. no. 103113), CD11b-BV421 (cat. no. 101235), F4/80-APC (cat. no. 123115), CD206-PE (cat. no. 141705), PE-IgG2a, k isotype control (cat. no. 400211), CD3-FITC (cat. no. 100203), CD4-BV421 (cat. no. 100437), and CD8a-APC (cat. no. 100711) were purchased from BioLegend. Viability was assessed by Zombie Aqua Fixable Viability Kit (cat. no. 423101) purchased from BioLgend. Unspecific antibody binding to Fc-receptors was avoided by using mouse FcR blocking reagent (1:10; Miltinyi Biotec, 130-092-575). Samples were washed and stained for 30 minutes at 4°C, washed and resuspended in 100 μL FACS buffer for acquisition. All flow cytometry was performed on either the BD Biosciences FACSCanto or the ACEA NovoCyte Quanteon. Data were analyzed using FlowJo version 10.6 software. Overview of the gating strategy can be found in Supplementary Fig. S1.

IHC

For IHC and immunofluorescence, MCA205 tumors were collected from tumor-bearing C57BL/6 mice and fixed in 1% paraformaldehyde for 1 hour and frozen in a cryo-embedding medium (OCT; Bio-Optica, cat. no. 05-9801). Frozen sections were cut, and 5-μm slides were fixed in ice-cold acetone for 10 minutes and incubated with rabbit polyclonal antiarginase I (1:50; Santa Cruz, cat. no. sc20150) overnight, or rabbit monoclonal anti-CD3 (1:150, Abcam; cat. no. ab16669) for 1 hour. For immunofluorescence, primary antibody incubation was followed by secondary goat antirabbit Alexa Fluor 546 (1:500; Invitrogen, cat. no. A11010), and nuclei were stained with Dapi (Sigma; cat. no. D9542). Image acquisition was performed using Zeiss LSM 800 confocal microscope. ARG1 intensity was expressed as arithmetic mean intensity measured with Zen 2.3 Lite software and was evaluated on digital images (5×400 microscopic fields per sample). For IHC, primary antibody incubation was followed by secondary goat antirabbit (1:500; Jackson Immuno Research, cat. no. 111-065-144), and immunoreactive antigens were detected using streptavidin peroxidase (Thermo Scientific; cat. no. TS-125-HR) and the DAB Chromogen System (Dako; cat. no. K3468). The number of $CD3^+$ cells was evaluated on digital images ($3–5 \times 200$ microscopic fields per sample), acquired with Leica DMRD optical microscope (Leica).

Immunosuppression assay

Immunosuppressive activity of myeloid cells isolated from tumor-bearing mice was evaluated as previously described (19). Briefly, spleen-derived $CD11b^+$ cells were isolated from MCA205 tumor–bearing mice by immunomagnetic sorting using CD11b Microbeads (Miltenyi Biotec) according to the manufacturer's instructions, and their purity was evaluated by flow cytometry. For all separations, the positive fraction was obtained with a purity of ≥ 95%. Purified $CD11b^+$ cells were cocultured at different concentration in presence of $CD45.2^+$ splenocytes from OT-I transgenic mice (Jackson Laboratories), labeled with 1 μmol/L CellTrace (Thermo Fisher Scientific) and diluted 1:10 with $CD45.1^+$ splenocytes (Jackson Laboratories), in the presence of OVA peptide (1 μg/mL final concentration). After 3 days of coculture, cells were stained with APC-Cy7-conjugated anti-CD45.2 (clone 104, eBioscience, Thermo Fisher Scientific) and PerCP-Cy5.5-conjugated anti-CD8 (clone SK1, eBioscience, Thermo Fisher Scientific). CellTrace signal of gated lymphocytes was used to analyze cell proliferation. Samples were acquired with the BD Biosciences FACSCanto II, and data were analyzed using the FlowJo software.

Liver enzyme measurements

C57BL/6 mice received four subcutaneous ARG1 peptide vaccination (as preciously described). Thirty-six days after the last vaccination, the mice were decapitated, and approximately 500 μL blood was collected in a 1-mL Eppendorf tube. Samples were left 30 minutes at room temperature to allow for blood coagulation. Samples were centrifuged for 10 minutes at $2000 \times g$. Sera (around 100–500 μL) were collected and stored at −20°C. Sera were tested with two kits: AST Activity Assay kit (Sigma-Aldrich, cat. no. MAK055-1KT) and ALT Activity Assay kit (Sigma-Aldrich, cat. no. MAK052-1KT) according to the manufacturer's protocols.

Statistical analysis

ELISPOT data were analyzed using the distribution-free resampling (DFR) method (20). For analysis of triplicates DFR, $P < 0.05$ (*) and DFRx2, $P < 0.01$ (**) were considered statistically significant. Analysis of flow cytometry data and ALT/AST levels was performed using Welch unpaired *t* tests. Antitumor effects over time were analyzed by using a mixed-effects model, whereas antitumor effects on specific

times points were analyzed using Welch unpaired *t* test. Survival curves were analyzed using the log-rank (Mantel–Cox) test. An event in the survival data was determined as the maximum tumor size allowed by the Danish Ethics Committee for these studies (864 mm^3 or 1,500 mm^3). Error bars denote the SEM. The DFR analysis was performed in RStudio (RStudio Team (2019). RStudio: Integrated Development for R. RStudio, Inc.; http://www.rstudio.com/), and all other statistical analyses were performed using the GraphPad Prism 9.0.0 software. Sample sizes were chosen based on power calculations from pilot experiments.

Results

ARG1-derived peptide vaccination leads to expansion of antigen-specific immune responses without inducing toxicity

We first examined the immunogenicity of two previously identified 20 amino acid long peptides ($ARG1_{261–280}$ and $ARG1_{191–210}$; ref. 15) after one vaccination with the individual peptides. $ARG1_{191–210}$ is derived from the human ARG1 sequence but only differs in one amino acid (R_{205} to L_{205} substitution in murine sequence), whereas $ARG1_{261–280}$ is conserved in both humans and mice. Upon vaccination with $ARG1_{261–280}$ or $ARG1_{191–210}$, we examined *ex vivo* IFNγ responses by ELISPOT assay (**Fig. 1A**). C57BL/6 mice vaccinated with the $ARG1_{261–280}$ peptide showed a significant $ARG1_{261–280}$-specific release of IFNγ (**Fig. 1B**), as well as BALB/c mice vaccinated with $ARG1_{191–210}$ peptide, which showed a significant release of IFNγ to $ARG1_{191–210}$ (**Fig. 1C**). To initially assess the impact of vaccination in controlling tumor growth, MCA205 tumor–bearing mice were vaccinated with $ARG1_{261–280}$ and $ARG1_{191–210}$ peptide in two different adjuvant settings, e.g., Montanide or anti-CD40 in combination with imiquimod (hereafter indicated as Covax; ref. 21). We found that ARG1-specific IFNγ responses were independent of the vaccine adjuvant and ARG1 epitopes (Supplementary Fig. S2) almost in all C57BL/6 ($H\text{-}2^b$) mice, even though only one epitope predicted to bind to $H\text{-}2^b$ showed measurable immune responses (Supplementary Fig. S3). Thus, we decided to focus on the two long $ARG1_{261–280}$ and $ARG1_{191–210}$ peptides. To further characterize $ARG1_{261–280}$-specific immune responses, $CD4^+$ and $CD8^+$ T cells were isolated from splenocytes of vaccinated mice by magnetic bead sorting and evaluated for their ability to release IFNγ in presence with ARG1-derived peptide by ELISPOT assay (**Fig. 1D**). The phenotype of the sorted fractions was confirmed using flow cytometry (Supplementary Fig. S1). In all analyzed mice, $CD4^+$ T cells secreted more IFNγ compared with $CD8^+$ T cells (**Fig. 1E**). Despite ARG1-specific IFNγ responses, the

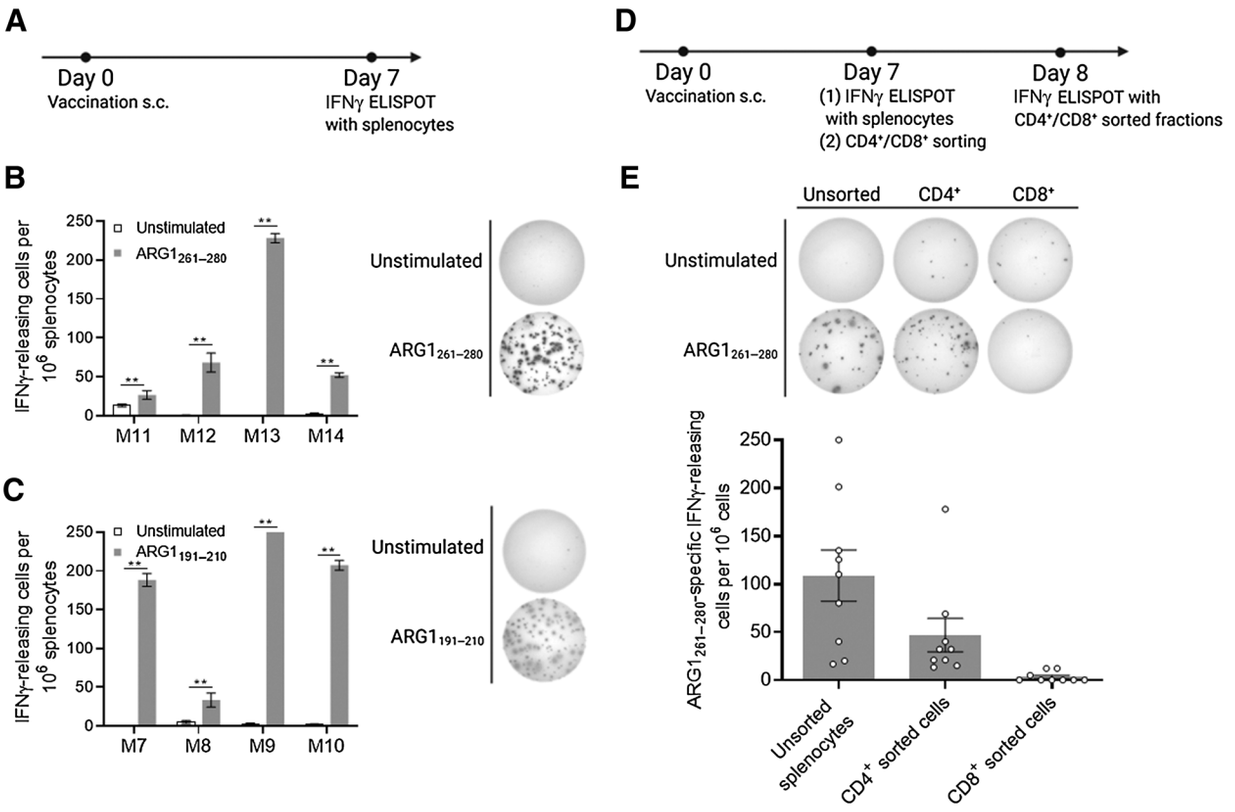

Figure 1.

ARG1-specific immune responses of vaccinated mice in the $CD4^+$ T-cell compartment. **A,** Experimental timeline for subcutaneous (s.c.) vaccination with ARG1 peptides and IFNγ ELISPOTs performed with splenocytes. **B,** Representative ELISPOTs and cumulative data showing IFNγ responses with and without stimulation from four C57BL/6 mice vaccinated with the $ARG1_{261–280}$ peptide. **C,** Representative ELISPOTs and cumulative data showing IFNγ responses with and without stimulation from four BALB/c mice vaccinated with the $ARG1_{191–210}$ peptide. M9 peptide-stimulated: too numerous to count. **D,** Experimental timeline for ELISPOTs using sorted $CD4^+/CD8^+$ cell fractions from ARG1 peptide–vaccinated mice. **E,** Representative ELISPOTs and cumulative data showing normalized IFNγ responses from unsorted, $CD4^+$ sorted fractions (fraction purity: 93.7–97.7%), and $CD8^+$ sorted fractions (fraction purity: 86.2–98.9%) with and without stimulation from C57BL/6 mice vaccinated with $ARG1_{261–280}$ peptide ($n = 9$). For ELISPOT data: DFR, $^*P < 0.05$; DFRx2, $^{**}P < 0.01$. All vaccinations were performed with Montanide as adjuvant.

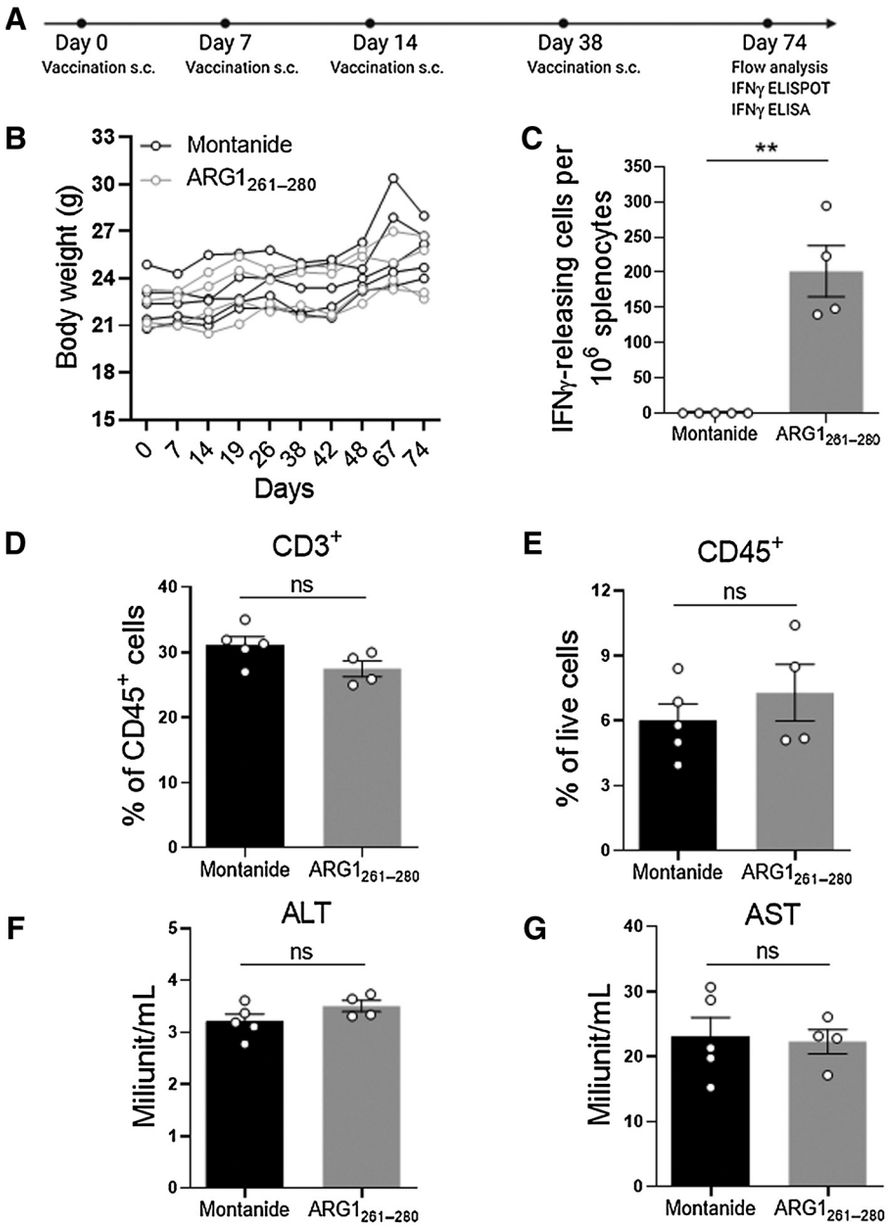

Figure 2.

ARG1 vaccinations are not associated with systemic toxicity. **A,** Experimental timeline for primary and boosting subcutaneous (s.c.) vaccinations with ARG1 peptides with and without anti–PD-1 therapy. **B,** Mouse weight over time. **C,** ELISPOTs: normalized IFNγ responses in splenocytes of $ARG1_{261–280}$ or control vaccinated mice upon stimulation with $ARG1_{261–280}$ peptide or DMSO as a control ($P = 0.0079$). For ELISPOT data: DFR, *, $P < 0.05$; DFRx2, **, $P < 0.01$. Flow analysis of $CD3^+$ (**D**) and $CD45^+$ (**E**) cells in the liver of $ARG1_{261–280}$ or control vaccinated mice. ALT (**F**) and AST (**G**) liver enzyme levels in the blood of $ARG1_{261–280}$ or control vaccinated mice determined by ELISA. All experiments performed on the same vaccinated C57BL/6 mice ($n = 9$ $ARG1_{261–280}$, $n = 10$ Montanide). All vaccinations were performed with Montanide. ns, not significant.

vaccines did not associate with any detectable systemic toxicity, as vaccinated mice did not show weight loss over time, no increased immune activity in the liver, or aberrant levels of liver enzymes in the blood were detected (**Fig. 2A–G**).

Immunization against ARG1 induces antitumor immunity as monotherapy and enhances the therapeutic efficacy of checkpoint immunotherapy

To assess the therapeutic effectiveness of $ARG1_{261–280}$ vaccination in tumor-bearing mice, we evaluated two different cancer settings (**Fig. 3**). In both models, tumor cells were subcutaneously injected on day 0 prior to the first weekly vaccination. Melanoma (B16-F10) and colon adenocarcinoma (MC38) mice vaccinated with $ARG1_{261–280}$ had significantly reduced tumor growth compared with the control groups (B16-F10: $P = 0.0001$, MC38: $P = 0.0098$; **Fig. 3**; Supplementary Fig. S4A and S4B), and increased infiltration of $CD4^+$ T cells was found in MC38 tumors of vaccinated mice compared with the control group (**Fig. 3E**).

Monoclonal anti–PD-1 has previously been shown to be functional in the MC38 mouse tumor model as monotherapy (22–24). Thus, we examined the combination of anti–PD-1 therapy and $ARG1_{261–280}$ vaccination in the MC38 cancer model. MC38 cells were inoculated prior to the first weekly vaccination with $ARG1_{261–280}$, and anti–PD-1 therapy was initiated on day 7. Both therapies were administered three times (**Fig. 4A**). Combination therapy with $ARG1_{261–280}$ vaccinations and anti–PD-1 therapy showed increased antitumor effects ($P = 0.0001$; **Fig. 4B**; Supplementary Fig. S4C) compared with either monotherapy with anti–PD-1 or $ARG1_{261–280}$ vaccination. The

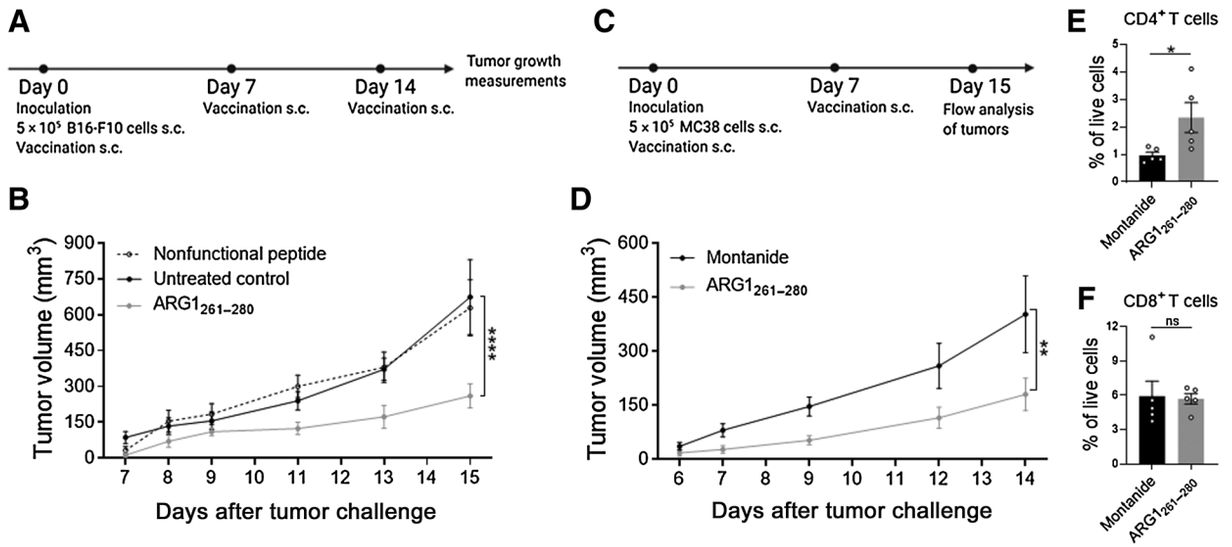

Figure 3.

ARG1 vaccination induces antitumor immunity as a monotherapy in syngeneic murine tumor models. **A,** Experimental timeline for the C57BL/6 syngeneic B16-F10 tumor model. sc, subcutaneous. **B,** Average B16-F10 tumor growth for the different treatment groups. $ARG1_{261–280}$ vaccination, $n = 6$; nonfunctional peptide vaccination, $n = 7$; no vaccination, $n = 16$. Comparison of $ARG1_{261–280}$ vaccinated group with no vaccination group, $P = 0.0001$. **C,** Experimental timeline for the C57BL/6 syngeneic MC38 tumor model. **D,** Average MC38 tumor growth for the two treatment groups ($n = 15$/group). Comparison of the $ARG1_{261–280}$ vaccinated group with control vaccinated group, $P = 0.0098$. Flow analysis of $CD4^+$ T cells (**E**; $P = 0.0395$) and $CD8^+$ T cells (**F**) in the MC38 tumors on day 15 after tumor inoculation ($n = 5$/group, chosen according to median tumor size). All vaccinations performed with Montanide. ns, not significant.

combination therapy also significantly increased the survival of tumor-bearing mice ($P = 0.0042$; **Fig. 4C**).

To understand the cellular mechanisms underlying this observed therapeutic combination effect, we analyzed the immune cell composition of the microenvironment. $ARG1_{261–280}$ vaccinations induced tumor infiltration of $CD45^+$ cells both as a monotherapy and in combination with anti–PD-1 (**Fig. 4D**). The combination therapy also induced a significant ARG1-dependent increase in the ratio of M1-like macrophages to M2-like macrophages (**Fig. 4E**), thus indicating a shift from an immunosuppressive to a more proinflammatory tumor microenvironment.

The therapeutic effectiveness of anti–PD-1 therapy in combination with $ARG1_{261–280}$-based vaccination was confirmed in a different tumor setting using an anti–PD-1–sensitive sarcoma model (MCA205). MCA205 tumor–bearing mice were vaccinated 3 days after tumor challenge. On day 7, mice were boosted with ARG1 vaccine, whereas anti–PD-1 treatment was infused by four iterative intraperitoneal administrations every second day (**Fig. 4F**), as previously described (25). $ARG1_{261–280}$-based immunization partially controlled tumor progression without inducing a significant increase in the survival in tumor-bearing mice (**Fig. 4G** and **H**; Supplementary Fig. S4D). On the contrary, the combination of ARG1 vaccination with anti–PD-1 showed a therapeutic synergy, promoting both increased antitumor efficacy and significantly prolonged survival (**Fig. 4G** and **H**). To elucidate the impact of ARG1 vaccine on the myeloid compartment, an immunosuppression assay (19) was conducted. $CD11b^+$ cells, containing immunosuppressive MDSCs, were purified from splenocytes of either vaccinated or unvaccinated tumor-bearing mice and cocultured *in vit*ro at different cell ratios with cell-trace–labeled OT1 splenocytes in the presence of immunodominant OVA peptide (19). The immunoregulative properties of $CD11b^+$ cells isolated from vaccinated mice were significantly impaired compared with cells from controls ($P < 0.036$), suggesting a potential reduction in ARG1-expressing myeloid cells by our developed immunization (**Fig. 4I**).

To further confirm the effectiveness of ARG1-based vaccination on controlling tumor progression, we also tested the $ARG1_{191–210}$-based vaccine in combination with anti–PD-1 treatment in the MCA205 tumor setting (**Fig. 5A**). In agreement with the previous results, the $ARG1_{191–210}$ vaccinations showed a direct antitumor effect compared with control groups and a similar therapeutic synergism in combination with anti–PD-1 treatment (**Fig. 5B**; Supplementary Fig. S4E). To investigate whether ARG1 targeting could be sufficient to reprogram the tumor framework, we evaluated tumor-infiltrating cells using IHC. We observed not only an increase in $CD3^+$ T cells (**Fig. 5C** and **D**) in the $ARG1_{191–210}$ vaccination group compared with control groups, but an overall significant reduction in $ARG1^+$ expression (**Fig. 5C** and **E**). In order to ensure that the antitumor effect was not limited to the C57BL/6 background, the same study was performed in the CT26 colon carcinoma model in BALB/c mice. Hemagglutinin (HA) peptide-based vaccination was utilized as a control. Similar antitumor effects by $ARG1_{191–210}$ vaccinations as monotherapy, as well as the synergy of the combination with anti–PD-1 treatment, were evident (**Fig. 5A** and **F**; Supplementary Fig. S4F).

The combined treatment of ARG1 vaccinations and anti–PD-1 therapy induces a protective memory immune response

The therapeutic combination of the $ARG1_{261–280}$-based vaccine and anti–PD-1 (**Fig. 4B** and **C**) resulted in complete tumor regression in several of the mice. To study whether the treatment had induced protective memory responses in these mice, they were rechallenged with 5×10^5 MC38 tumor cells on the left flank on day 51 after primary tumor inoculation and treatment initiation (**Fig. 6A**). As a control to the rechallenge group, seven tumor- and treatment-naïve mice were inoculated with MC38 cells on the left flank. None of the mice were

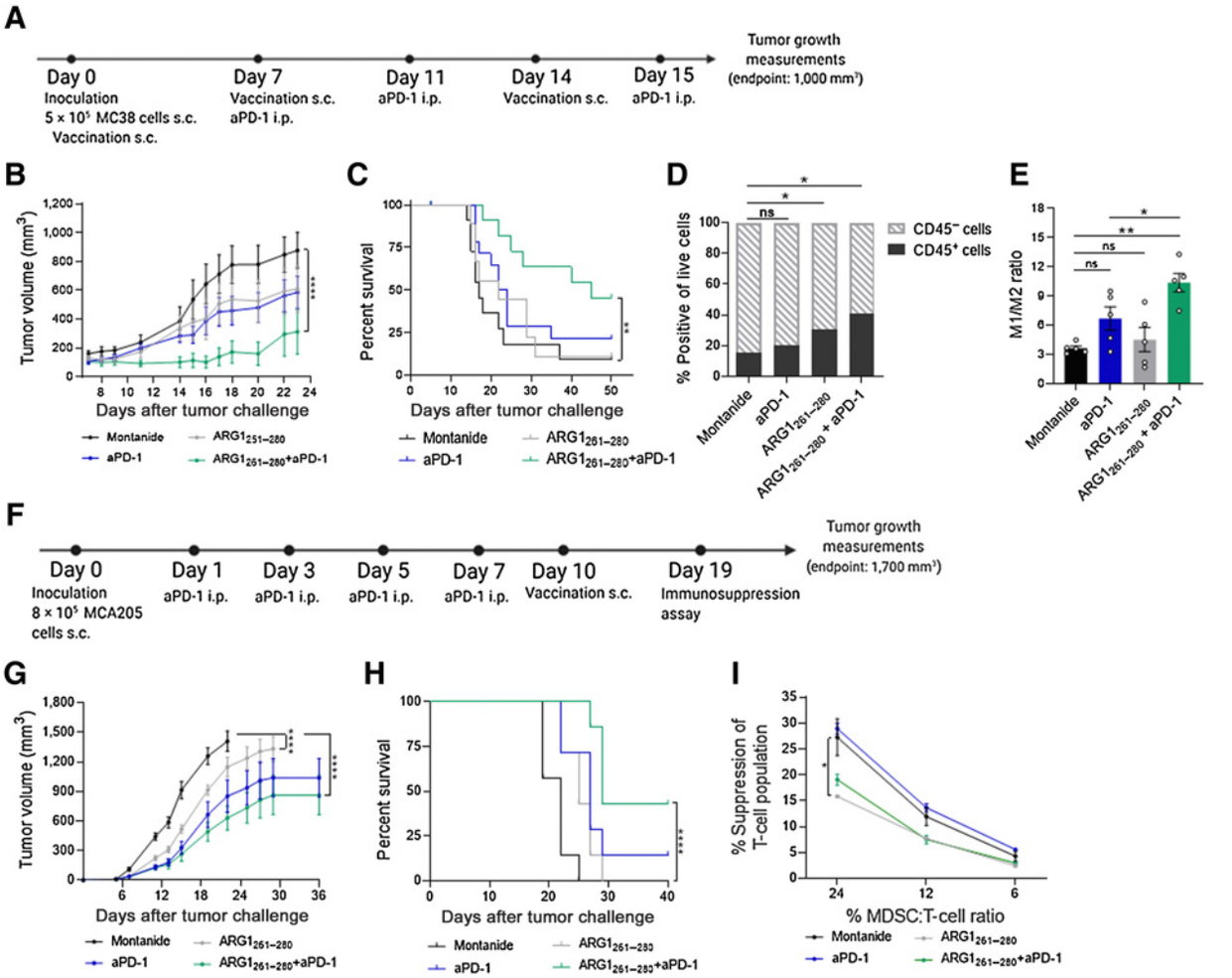

Figure 4.

Effective combination of ARG1 vaccination and anti–PD-1 therapy induces antitumor effects, prolongs survival, and induces proinflammatory changes in the tumor microenvironment. **A,** Experimental timeline for the C57BL/6 syngeneic MC38 tumor model with three weekly $ARG1_{261–280}$ vaccinations and three anti–PD-1 treatments. i.p., intraperitoneal; s.c., subcutaneous. **B,** Average MC38 tumor growth for the four treatment groups ($n = 15$/group). Comparison of combination group with the control vaccinated group, $P = 0.0001$. **C,** Survival over time. Comparison of combination group with the control vaccinated group, $P = 0.0042$. Flow analysis of $CD45^{+/-}$ cells (**D**) and the ratio of M1 (MMR^{-}) to M2 (MMR^{+}) macrophages (**E**) in the MC38 tumors on day 10 after tumor inoculation ($n =$ 5/group, chosen according to median tumor size). **F,** Experimental timeline for the C57BL/6 syngeneic MCA205 tumor model treated as indicated. **G,** Average MCA205 tumor growth for the four treatment groups ($n = 12$/group). Comparison of $ARG1_{261–280}$ with control vaccinated, $P < 0.0001$; $ARG1_{261–280}$ + anti–PD-1 with control vaccinated, $P < 0.0001$. Five mice were euthanized for flow analysis on day 19, and seven mice were continued for a survival study. **H,** Survival over time. Comparison of $ARG1_{261–280}$ + anti–PD-1 with control vaccinated, $P \leq 0.0001$. **I,** Immunosuppression assay at three different MDSC:T-cell ratios. Comparison of the $ARG1_{261–280}$ group with Montanide control at 24% MDSCs, $P < 0.036$. All vaccinations performed with Montanide. ns, not significant.

treated during the tumor rechallenge. Seven days following rechallenge initiation, tumors were measurable on all controls, whereas none of the rechallenged mice developed tumors (**Fig. 6B**; Supplementary Fig. S4G). Mice that cleared tumors were followed until day 185 after primary tumor inoculation, and spleens and draining lymph nodes were collected for IFNγ ELISPOT. Results showed a significant ARG1-specific IFNγ release in three of five mice treated with the combination therapy in the draining lymph nodes (**Fig. 6C**) and in the spleens of all mice treated with the combination therapy (**Fig. 6D**). Supernatants were collected from the ELISPOT cultures, and IFNγ ELISAs showed a significant release of IFNγ upon stimulation with the $ARG1_{261–280}$ peptide in all mice treated with the combination therapy (**Fig. 6E**).

Discussion

In the current study, we examined the antitumor effect of ARG1-targeting vaccines in four different *in vivo* models of cancer. We showed that it was possible to induce $CD4^{+}$ T-cell response against a peptide derived from ARG1 after just a single immunization using a simple vaccine based on a long peptide mixed with an adjuvant. We described that vaccinations with the $ARG1_{261–280}$ epitope had a significant antitumor effect on the growth of B16-F10 tumors, as well as MC38 tumors, and we also found an increase in $CD4^{+}$ T cells in the tumor microenvironment in ARG1 peptide–vaccinated mice. In line with these results, we found increased $CD3^{+}$ T-cell infiltration and decreased ARG1 expression in MCA205 tumors upon vaccination with the $ARG1_{191–210}$ epitope mixed with adjuvant. The antitumor

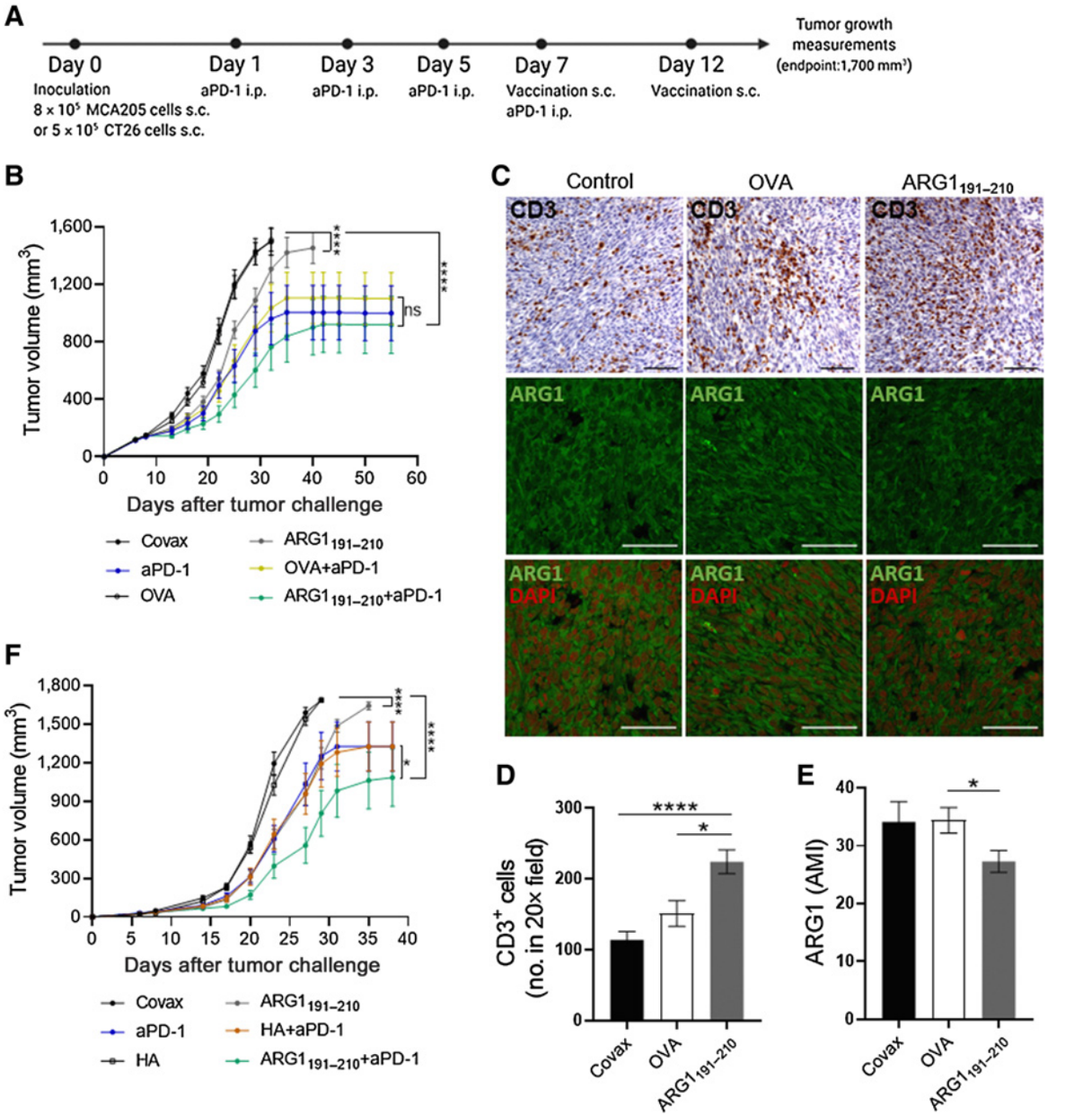

Figure 5.

The $ARG1_{191–210}$ peptide-based vaccine enhances the therapeutic efficacy of checkpoint immunotherapy. **A,** Experimental timeline for the C57BL/6 syngeneic MCA205 and the BALB/c syngeneic CT26 tumor models. 250 μg of anti–PD-1 was administered per mouse per injection. Covax was used as the vaccine adjuvant. i.p. intraperitoneal; s.c., subcutaneous. **B,** Average MCA205 tumor growth for the different treatment groups ($n = 15$/group). Comparison of $ARG1_{191–210}$ + anti–PD-1 with Covax control, $P < 0.0001$; $ARG1_{191–210}$ + anti-PD-1 with OVA, $P < 0.0001$; $ARG1_{191–210}$ + anti-PD-1 with OVA + anti-PD-1, $P = 0.073$; $ARG1_{191–210}$ with Covax control, $P < 0.0001$; $ARG1_{191–210}$ with OVA, $P < 0.0001$. **C,** IHC or immunofluorescence for ARG1 in MCA205 tumors. Scale bar, 100 μm. **D,** Quantification of IHC of $CD3^+$ cells ($n = 3$ tumors/group) from **C**. Comparison of $ARG1_{191–210}$ with Covax control, $P < 0.0001$; $ARG1_{191–210}$ with OVA control, $P < 0.011$. **E,** Quantification of immunofluorescence (AMI, arithmetic mean intensity) of ARG1 expression on tumors from **C** ($n = 4$ tumors/group). Comparison of $ARG1_{191–210}$ with OVA control, $P < 0.0430$. **F,** Average CT26 tumor growth of the different treatment groups ($n = 14$/group). Comparison of $ARG1_{191–210}$ + anti–PD-1 with Covax control, $P < 0.0001$; $ARG1_{191–210}$ + anti-PD-1 with HA, $P < 0.0001$; $ARG1_{191–210}$ + anti–PD-1 with HA + anti–PD-1, $P < 0.0108$; $ARG1_{191–210}$ with Covax control, $P < 0.0001$; $ARG1_{191–210}$ with HA $P < 0.0001$. All vaccinations performed with Covax. ns, not significant.

effects of the $ARG1_{191–210}$-based vaccination were also evident in CT26 tumor–bearing mice with BALB/c background. Thus, the therapeutic and immunomodulatory effects of ARG1-targeting immunotherapy are independent of genetic background and cancer type, which allows us to speculate that this approach could be a broadly applicable treatment in different cancer settings. ARG1 expression is one of the main characteristics of both MDSCs and TAMs. ARG1-expressing myeloid cells play a major role in the development of a suppressive

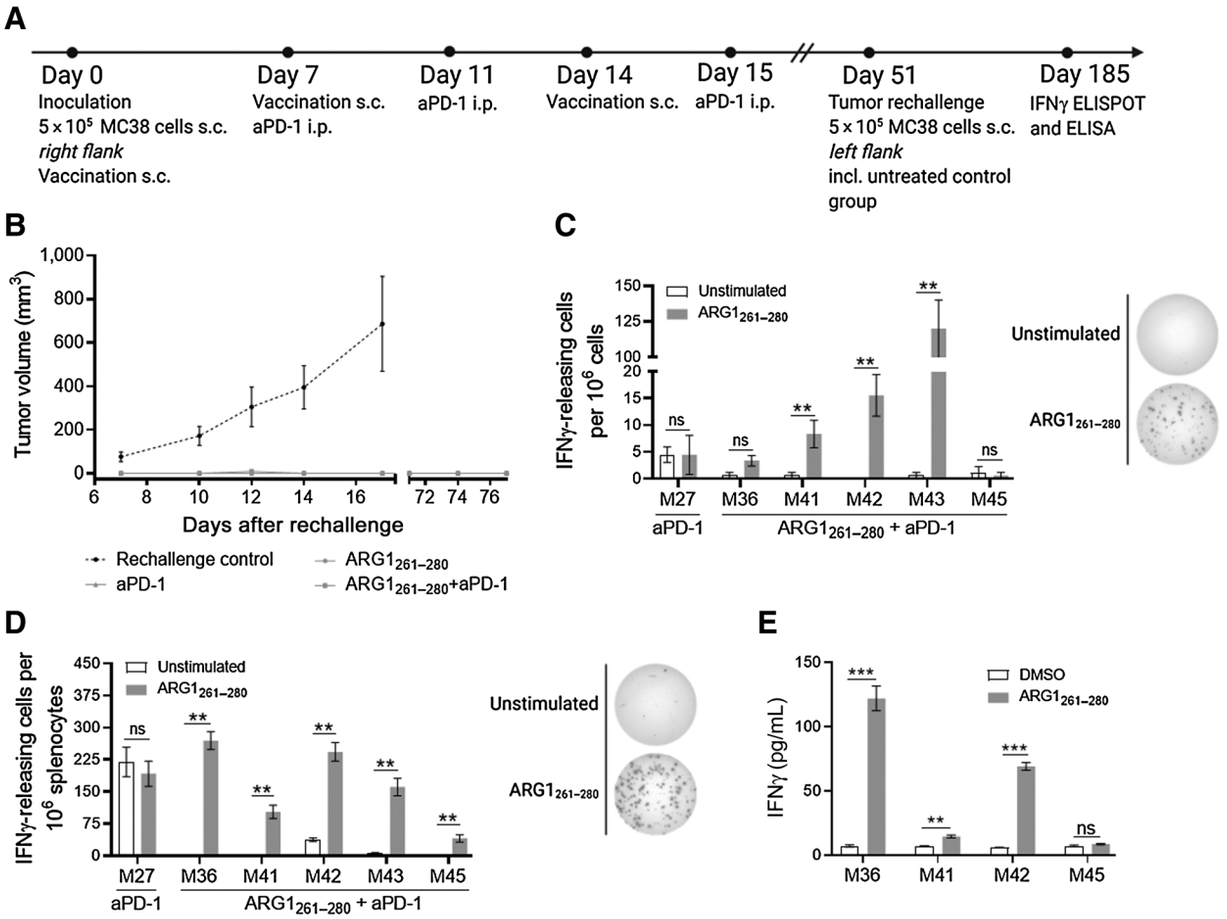

Figure 6.

Effective combination therapy of ARG1 vaccinations and anti–PD-1 therapy induces a protective memory immune response in long-term survivors. **A,** Experimental timeline of vaccination and anti–PD-1 treatment in the MC38 tumor model. i.p. intraperitoneal; s.c., subcutaneous. **B,** Average MC38 tumor growth of surviving mice ($ARG1_{261–280}$, $n = 1$; anti–PD-1, $n = 3$; $ARG1_{261–280}$ + anti–PD-1, $n = 6$) and rechallenge control ($n = 7$) after tumor rechallenge on opposite flank. **C,** Representative ELISPOTs and IFNγ responses in the draining lymph nodes of surviving mice (anti–PD-1, $n = 1$; $ARG1_{261–280}$ + anti–PD-1, $n = 5$) upon stimulation with $ARG1_{261–280}$ peptide. For ELISPOT data: DFR, *, $P < 0.05$; DFRx2, **, $P < 0.01$. **D,** Representative ELISPOTs and IFNγ responses in splenocytes of surviving mice (anti–PD-1, $n = 1$; $ARG1_{261–280}$ + anti–PD-1, $n = 5$) upon stimulation with $ARG1_{261–280}$ peptide. **E,** Splenocytes were restimulated *in vitro* with $ARG1_{261–280}$ peptide or DMSO as a control, and supernatants were collected for IFNγ ELISAs. All vaccinations performed with Montanide. ns, not significant.

microenvironment, as they prevent effector lymphocyte proliferation at the tumor site (4, 26, 27). We previously described that ARG1-specific proinflammatory T cells are naturally occurring in the memory T-cell repertoire of the human immune system (17). We described that such T cells were naturally activated in T_H2 cytokine environments mimicking a tumor microenvironment (28). Hence, ARG1-specific T cells expanded in response to IL4 without any other specific stimulation. ARG1-specific T cells that release IFNγ in response to an ARG1-expressing M2 macrophages may therefore drive the immune response away from T_H2 and back into the T_H1 pathway. Here, we expanded these finding by describing that the activation of ARG1-specific T cells by peptide vaccines can directly be used to modulate the tumor microenvironment. We also previously reported the existence of other autoreactive, antigen-specific proinflammatory T cells [defined as antiregulatory T cells (anti-Tregs); ref. 29] that can react to immunosuppressive cells and therefore are able to counteract the many different immunosuppressive feedback mechanisms mediated by such regulatory cells. Hence, we have characterized anti-Tregs, which specifically recognize HLA-restricted epitopes derived from proteins expressed in regulatory immune cells, e.g., indoleamine 2,3-dioxygenase (IDO; refs. 30–33), IDO2 (34), tryptophan 2,3-dioxygenase (35), programmed death-ligand 1 (PD-L1; refs. 36–39), CCL22 (40), arginase 2 (ARG2; ref. 41), in addition to ARG1 (15–17) epitopes.

We previously described the existence of proinflammatory effector T cells that recognize ARG2 (41), and ARG2 is, therefore, also a potential target for novel immune modulatory vaccines. We do not yet know, however, if ARG2, like ARG1, can be utilized as a target for anticancer vaccinations. Because ARG1 and ARG2 are expressed heterogeneously, the combination of ARG1 and ARG2 for vaccination might capture different immunosuppressive arginase-expressing cells in the tumor microenvironment and benefit more patients. Activation of ARG1-specific T cells with a vaccination differentiates from other ways of targeting ARG1 in a cancer setting by its immunomodulatory effects, as it should cause T-cell infiltration at the tumor site converting an immunosuppressive environment into a proinflammatory

environment. Thus, in contrast to ARG1 pharmacologic inhibition, ARG1 vaccination combines both TAM depletion (especially if it successfully activates ARG1-specific $CD8^+$ T cells) and TAM reprogramming (42, 43) by introducing proinflammatory cytokines, such as IFNγ, into the immunosuppressive microenvironment. Indeed, we found that not only the lymphoid compartment was affected by the vaccines, but also the myeloid compartment, as the MDSCs in the tumor microenvironment were less immunosuppressive upon vaccination with $ARG1_{261–280}$. Accordingly, this rebalancing should increase the effect of T-cell–enhancing drugs, like immune-checkpoint blockers. MDSCs are under the influence of hypoxia-inducible factor 1 alpha (HIF1α) and A2 adenosine receptor (A2AR)–mediated immunosuppressive transcription and signaling. These are among the most important mechanisms used by MDSCs to decrease antitumor immunity and contribute to tumor immune escape (44). Thus, synergistic combination of ARG1 vaccines with the blockade of the hypoxia A2AR immunosuppressive pathway (45–47) could be an interesting future treatment modality.

To avoid immune-mediated clearance, advanced tumors exploit an array of immune suppressive pathways. These pathways are unlikely to be overcome when only interfering with signaling checkpoints (48, 49). We showed that ARG1 vaccination synergizes with anti–PD-1 therapy in multiple *in vivo* tumor models. TAM infiltration in the tumor microenvironment has been described as a major reason that checkpoint blockers show limited effects in most patients with cancer (50–54). ARG1-targeting vaccination induces a T_h1-associated inflammation that favors the expression of certain immune-related molecules such as PD-L1 in both cancer, immune, and stroma cells. Therefore, this immunotherapeutic approach could generate a microenvironment more sensitive to anti–PD-1/PD-L1 blockade therapy, as well as a long-term protective memory immune response as described in this study.

In conclusion, we demonstrated that an ARG1-targeting vaccine can activate the endogenous antitumor immunity in synergy with checkpoint blockade through the induction of a robust shift toward a more proinflammatory microenvironment, but without the development of systemic toxicity in the host. We previously showed similar effects of another immune modulatory vaccine based on epitopes from IDO with Montanide in a mouse setting (55). Promising clinical efficacy has been reported in a nonrandomized phase I/II study with IDO/PD-L1 peptide vaccines with Montanide, in combination with nivolumab, in patients with progressive metastatic melanoma (ClinicalTrials.gov; NCT03047928, abstract published; ref. 56). Hence, combining these peptide vaccines with checkpoint blockade therapy may be the new general way forward in treating many different cancer patients. We are currently examining the safety and immunologic effect of ARG1-derived vaccines with Montanide in two early vaccination trials at our institution (ClinicalTrials.gov: NCT03689192, NCT04051307).

Authors' Disclosures

M. Aaboe Jørgensen reports grants from Copenhagen University Hospital, Herlev, and Danish Council for Independent Research during the conduct of the study. E. Martinenaite reports grants from Innovation Fund Denmark during the conduct of the study. M. Zocca reports personal fees from Valo Therapeutics and nonfinancial support from Unikum Therapeutics outside the submitted work. V. Bronte reports grants and personal fees from IO Biotech during the conduct of the study. M.H. Andersen reports grants and personal fees from IO Biotech during the conduct of the study; grants and personal fees from IO Biotech outside the submitted work; and a patent for immunogenic arginase peptides pending to IO Biotech, a patent for arginase 1 polypeptides pending to IO Biotech, and a patent for immunogenic arginase 2 polypeptides pending to IO Biotech. No disclosures were reported by the other authors.

Disclaimer

The funders had no role in the study design, collection of data, data analysis, decision to publish, or manuscript preparation.

Authors' Contributions

M. Aaboe Jørgensen: Data curation, formal analysis, investigation, writing–original draft, project administration. **S. Ugel:** Data curation, formal analysis, investigation, writing–review and editing. **M. Linder Hübbe:** Investigation, writing–review and editing. **M. Carretta:** Supervision, investigation. **M. Perez-Penco:** Investigation. **S.E. Weis-Banke:** Investigation. **E. Martinenaite:** Investigation, writing–review and editing. **K. Kopp:** Investigation. **M. Chapellier:** Investigation. **A. Adamo:** Investigation. **F. De Sanctis:** Investigation. **C. Frusteri:** Investigation. **M. Iezzi:** Investigation. **M.-B. Zocca:** Funding acquisition. **D. Hargbøll Madsen:** Data curation, supervision, writing–review and editing. **A. Wakatsuki Pedersen:** Supervision, writing–review and editing. **V. Bronte:** Supervision, funding acquisition, writing–review and editing. **M.H. Andersen:** Conceptualization, data curation, supervision, funding acquisition, writing–review and editing.

Acknowledgments

The authors thank Merete Jonassen for excellent technical support. This work was supported by Copenhagen University Hospital, Herlev, and the Danish Council for Independent Research.

The costs of publication of this article were defrayed in part by the payment of page charges. This article must therefore be hereby marked *advertisement* in accordance with 18 U.S.C. Section 1734 solely to indicate this fact.

Received April 19, 2021; revised June 14, 2021; accepted September 9, 2021; published first September 13, 2021.

References

1. Umansky V, Blattner C, Fleming V, Hu X, Gebhardt C, Altevogt P, et al. Myeloid-derived suppressor cells and tumor escape from immune surveillance. Semin Immunopathol 2017;39:295–305.
2. Schröder M, Loos S, Naumann SK, Bachran C, Krötschel M, Umansky V, et al. Identification of inhibitors of myeloid-derived suppressor cells activity through phenotypic chemical screening. Oncoimmunology 2017;6:34–6.
3. Karakhanova S, Link J, Heinrich M, Shevchenko I, Yang Y, Hassenp M, et al. Characterization of myeloid leukocytes and soluble mediators in pancreatic cancer: importance of myeloid-derived suppressor cells Svetlana. Oncoimmunology 2015;4:1–13.
4. Ugel S, De Sanctis F, Mandruzzato S, Bronte V. Tumor-induced myeloid deviation: when myeloid-derived suppressor cells meet tumor-associated macrophages. J Clin Invest 2015;125:3365–76.
5. Lang S, Bruderek K, Kaspar C, Höing B, Kanaan O, Dominas N, et al. Clinical relevance and suppressive capacity of human myeloid-derived suppressor cell subsets. Clin Cancer Res 2018;24:4834–44.
6. de Boniface J, Mao Y, Schmidt-Mende J, Kiessling R, Poschke I. Expression patterns of the immunomodulatory enzyme arginase 1 in blood, lymph nodes and tumor tissue of early-stage breast cancer patients. Oncoimmunology 2012;1:1305–12.
7. Rodriguez PC, Ernstoff MS, Hernandez C, Atkins M, Zabaleta J, Sierra R, et al. Arginase I–producing myeloid-derived suppressor cells in renal cell carcinoma are a subpopulation of activated granulocytes. Cancer Res 2009;69:1553–60.
8. Rotondo R, Barisione G, Mastracci L, Grossi F, Orengo AM, Costa R, et al. IL-8 induces exocytosis of arginase 1 by neutrophil polymorphonuclears in nonsmall cell lung cancer. Int J Cancer 2009;125:887–93.
9. Mondanelli G, Bianchi R, Pallotta MT, Orabona C, Albini E, Iacono A, et al. A relay pathway between arginine and tryptophan metabolism confers immunosuppressive properties on dendritic cells. Immunity 2017;46:233–44.
10. Rodriguez PC, Hernandez CP, Quiceno D, Dubinett SM, Zabaleta J, Ochoa JB, et al. Arginase I in myeloid suppressor cells is induced by COX-2 in lung carcinoma. J Exp Med 2005;202:931–9.

11. Steggerda SM, Bennett MK, Chen J, Emberley E, Huang T, Janes JR, et al. Inhibition of arginase by CB-1158 blocks myeloid cell-mediated immune suppression in the tumor microenvironment. J Immunother Cancer 2017;5:1–18.
12. Molon B, Ugel S, Del Pozzo F, Soldani C, Zilio S, Avella D, et al. Chemokine nitration prevents intratumoral infiltration of antigen-specific T cells. J Exp Med 2011;208:1949–62.
13. Serafini P, Meckel K, Kelso M, Noonan K, Califano J, Koch W, et al. Phosphodiesterase-5 inhibition augments endogenous antitumor immunity by reducing myeloid-derived suppressor cell function. J Exp Med 2006;203: 2691–702.
14. Marigo I, Zilio S, Desantis G, Mlecnik B, Agnellini AHR, Ugel S, et al. T cell cancer therapy requires CD40-CD40L activation of tumor necrosis factor and inducible nitric-oxide-synthase-producing dendritic cells. Cancer Cell 2016;30: 377–90.
15. Martinenaite E, Mortensen REJ, Hansen M, Holmström MO, Ahmad SM, Jørgensen NGD, et al. Frequent adaptive immune responses against Arginase-1. Oncoimmunology 2017;7:e1404215.
16. Jørgensen MA, Holmström MO, Martinenaite E, Riley CH, Hasselbalch HC, Andersen MH, et al. Spontaneous T-cell responses against Arginase-1 in the chronic myeloproliferative neoplasms relative to disease stage and type of driver mutation. Oncoimmunology. 2018;7:e1468957.
17. Martinenaite E, Ahmad SM, Svane IM, Andersen MH. Peripheral memory T cells specific for Arginase-1. Cell Mol Immunol 2019;16:781–9.
18. Madsen DH, Jürgensen HJ, Siersbæk MS, Kuczek DE, Grey Cloud L, Liu S, et al. Tumor-associated macrophages derived from circulating inflammatory monocytes degrade collagen through cellular uptake. Cell Rep 2017;21:3662–71.
19. Solito S, Pinton L, De Sanctis F, Ugel S, Bronte V, Mandruzzato S, et al. Methods to measure of MDSC immune suppressive activity in vitro and in vivo. Curr Protoc Immunol 2018;1–42.
20. Moodie Z, Price L, Gouttefangeas C, Mander A, Janetzki S, Löwer M, et al. Response definition criteria for ELISPOT assays revisited. Cancer Immunol Immunother 2010;59:1489–501.
21. Hailemichael Y, Dai Z, Jaffarzad N, Ye Y, Medina MA, Huang X-F, et al. Persistent antigen at vaccination sites induces tumor-specific CD8+ T cell sequestration, dysfunction and deletion. Nat Med 2013;19:465–72.
22. Ngiow SF, Young A, Jacquelot N, Yamazaki T, Enot D, Zitvogel L, et al. A threshold level of intratumor CD8+ T-cell PD1 expression dictates therapeutic response to anti-PD1. Cancer Res 2015;75:3800–11.
23. Selby MJ, Engelhardt JJ, Johnston RJ, Lu LS, Han M, Thudium K, et al. Preclinical development of ipilimumab and nivolumab combination immunotherapy: mouse tumor models, in vitro functional studies, and cynomolgus macaque toxicology. PLoS One 2016;11:1–19.
24. Deng L, Liang H, Burnette B, Beckett M, Darga T, Weichselbaum RR, et al. Irradiation and anti–PD-L1 treatment synergistically promote antitumor immunity in mice. J Clin Invest 2014;124:687–95.
25. Jacquelot N, Yamazaki T, Roberti MP, Duong CPM, Andrews MC, Verlingue L, et al. Sustained type I interferon signaling as a mechanism of resistance to PD-1 blockade. Cell Res 2019;29:846–61.
26. Gajewski TF, Schreiber H, Fu Y-X. Innate and adaptive immune cells in the tumor microenvironment. Nat Immunol Immunol 2013;14:1014–22.
27. Gabrilovich DI, Ostrand-Rosenberg S, Bronte V. Coordinated regulation of myeloid cells by tumours. Nat Rev Immunol 2012;12:253–68.
28. Martinenaite E, Ahmad SM, Bendtsen SK, Jørgensen MA, Weis-Banke SE, Svane IM, et al. Arginase-1-based vaccination against the tumor microenvironment: the identification of an optimal T-cell epitope. Cancer Immunol Immunother 2019;68:1901–7.
29. Andersen MH. Immune regulation by self-recognition: novel possibilities for anticancer immunotherapy. J Natl Cancer Inst 2015;107:1–8.
30. Munir S, Larsen SK, Iversen TZ, Donia M, Klausen TW, Svane IM, et al. Natural CD4 + T-cell responses against indoleamine 2,3-dioxygenase. PLoS One 2012;7: e34568.
31. Straten PT, Andersen MH. Possible benefits of the targeting of indoleamine 2,3-dioxygenase (IDO) in hepatitis B vaccination. Vaccine 2011;29:3728.
32. Sørensen RB, Hadrup SR, Svane IM, Hjortsø MC, Straten PT, Andersen MH. Indoleamine 2,3-dioxygenase specific, cytotoxic T cells as immune regulators. Blood 2011;117:2200–10.
33. Andersen MH. CD4 responses against IDO. Oncoimmunology 2012;1:1211–2.
34. Sørensen RB, Køllgaard T, Andersen RS, Van Den Berg JH, Svane IM, Straten PT, et al. Spontaneous cytotoxic T-cell reactivity against indoleamine 2,3-dioxygenase-2. Cancer Res 2011;71:2038–44.
35. Hjortsø MD, Larsen SK, Kongsted P, Met Ö, Frøsig TM, Andersen GH, et al. Tryptophan 2,3-dioxygenase (TDO)-reactive T cells differ in their functional characteristics in health and cancer. Oncoimmunology 2015;4:e968480.
36. Munir S, Andersen GH, Met Ö, Donia M, Frøsig TM, Larsen SK, et al. HLA-restricted CTL that are specific for the immune checkpoint ligand PD-L1 occur with high frequency in cancer patients. Cancer Res 2013;73:1764–76.
37. Munir S, Andersen G, Svane I, Andersen M. The immune checkpoint regulator PD-L1 is a specific target for naturally occurring $CD4^+$ T cells. Oncoimmunology 2013;2:e23991.
38. Munir S, Andersen G, Woetmann A, Ødum N, Becker J, Andersen M. Cutaneous T cell lymphoma cells are targets for immune checkpoint ligand PD-L1-specific, cytotoxic T cells. Leukemia 2013;27:2251–3.
39. Ahmad SM, Svane IM, Andersen MH. The stimulation of PD-L1-specific cytotoxic T lymphocytes can both directly and indirectly enhance antileukemic immunity. Blood Cancer J 2014;4:e230.
40. Martinenaite E, MA S, Hansen M, Ö M, Westergaard MW, Larsen SK, et al. CCL22-specific T cells: modulating the immunosuppressive tumor microenvironment. Oncoimmunology 2016;5:1–10.
41. Weis-Banke SE, Hübbe ML, Holmström MO, Jørgensen MA, Bendtsen SK, Martinenaite E, et al. The metabolic enzyme arginase-2 is a potential target for novel immune modulatory vaccines. Oncoimmunology 2020;9:1771142.
42. Duluc D, Corvaisier M, Blanchard S, Catala L, Descamps P, Gamelin E, et al. Interferon-γ reverses the immunosuppressive and protumoral properties and prevents the generation of human tumor-associated macrophages. Int J Cancer 2009;125:367–73.
43. Cassetta L, Pollard JW. Targeting macrophages: therapeutic approaches in cancer. Nat Rev Drug Discov 2018;17:887–904.
44. Hatfield SM, Kjaergaard J, Lukashev D, Schreiber TH, Belikoff B, Abbott R, et al. Immunological mechanisms of the antitumor effects of supplemental oxygenation. Sci Transl Med 2015;7:263–9.
45. Hatfield SM, Sitkovsky M. Oxygenation to improve cancer vaccines, adoptive cell transfer and blockade of immunological negative regulators. Oncoimmunology 2015;4:12–4.
46. Sitkovsky MV. Lessons from the A2A adenosine receptor antagonist– enabled tumor regression and survival in patients with treatment-refractory renal cell cancer. Cancer Discov 2020;10:16–9.
47. Hatfield SM, Sitkovsky MV. Antihypoxic oxygenation agents with respiratory hyperoxia to improve cancer immunotherapy. J Clin Invest 2020;130:5629–37.
48. Sharma P, Allison JP. The future of immune checkpoint therapy. Science 2015; 348:56–61.
49. Smyth MJ, Ngiow SF, Ribas A, Teng MWL. Combination cancer immunotherapies tailored to the tumour microenvironment. Nat Rev Clin Oncol. 2016;13: 143–58.
50. Allavena P, Mantovani A. Immunology in the clinic review series; focus on cancer: tumour-associated macrophages: undisputed stars of the inflammatory tumour microenvironment. Clin Exp Immunol 2012;167:195–205.
51. Mantovani A, Marchesi F, Malesci A, Laghi L, Allavena P. Tumor-associated macrophages as treatment targets in oncology. Nat Rev Clin Oncol 2017;14: 399–416.
52. Quaranta V, Schmid MC. Macrophage-mediated subversion of anti-tumour immunity. Cells. 2019;8:1–17.
53. Roccaro AM, Sacco A, Jimenez C, Maiso P, Moschetta M, Mishima Y, et al. C1013G/CXCR4 acts as a driver mutation of tumor progression and modulator of drug resistance in lymphoplasmacytic lymphoma. Blood 2014;123:4120–31.
54. De Palma M, Lewis CE. Macrophage regulation of tumor responses to anticancer therapies. Cancer Cell 2013;23:277–86.
55. Dey S, Sutanto-Ward E, Kopp KL, Duhadaway J, Mondal A, Ghaban D, et al. Peptide vaccination directed against IDO1-expressing immune cells elicits $CD8^+$ and $CD4^+$ T-cell-mediated antitumor immunity and enhanced anti-PD1 responses. J Immunother Cancer 2020;8:e000605.
56. Kjeldsen JW, Lorentzen CL, Martinenaite E, Svane I-M, Andersen MH. Clinical efficacy and immunity of combination therapy with nivolumab and IDO/PD-L1 peptide vaccine in patients with metastatic melanoma: a phase I/II trial. Ann Oncol 2020;31:S1176.